RESEARCH PAPER

Electro-Optical Properties of Cesium Lead Iodide: A Computational Approach

Md. Abdullah Al Asad[1,*], Hasan Ridoy[1], Md. Shuzon Ali[2], Mst. Jeba Maimuna[3]

* *dr.asad.eee@gmail.com*

[1] Department of Electrical and Electronic Engineering, Gopalganj Science and Technology University, Gopalganj, Bangladesh-8100
[2] Department of Mathematics, Gopalganj Science and Technology University, Gopalganj, Bangladesh-8100
[3] Department of Physics, Gopalganj Science and Technology University, Gopalganj, Gopalganj, Bangladesh-8100

Received: January 2025 **Revised: August 2025** **Accepted: September 2025**
DOI: 10.22068/ijmse.3898

Abstract: *Perovskite materials have garnered considerable attention in recent years due to their exceptional electro-optical properties, making them promising candidates for various applications in photovoltaics, light-emitting devices, and beyond. Among these perovskite materials, $CsPbI_3$ stands out as a notable example due to its remarkable stability, tunable bandgap, and efficient light-emitting properties. The crystal structure, composition, and introductory properties of $CsPbI_3$ perovskite are being focused on using density functional theory (DFT). In a detailed exploration of Electronic, Elastic, and Optical properties, Population analysis, and shedding light on the unique attributes of this material, this study highlights these attributes. To do the above computation, we have used CASTEP in Material Studio.*

Keywords: *$CsPbI_3$, Density functional theory, Structural properties, Electronic properties, Optical properties, Elasticity.*

1. INTRODUCTION

Perovskite materials have emerged as a pivotal class of materials, not only in the field of materials science but also in condensed matter physics, due to their remarkable optoelectronic properties and diverse applications. Among the various perovskite materials, $CsPbI_3$ has garnered significant attention as a talented candidate for applications in photovoltaics, light-emitting devices, and as a potential platform for fundamental research in solid-state physics. $CsPbI_3$ belongs to the family of lead halide perovskites, characterised by its unique properties, including optical, elastic, band structure, density of states, and population analysis, which have become crucial points of research in recent years [1]. $CsPbI_3$ perovskite materials exhibit intriguing electronic properties, including a direct bandgap and excellent charge carrier mobility. By considering the band structure and density of states, we can elucidate the charge transport mechanisms, which are pivotal for optimising device performance in electronic and optoelectronic applications [2]. The optoelectronic properties of $CsPbI_3$ perovskite materials are of specific interest because of their potential to revolutionize the field of photovoltaics. Their high absorption coefficients, tunable bandgap, and long carrier lifetimes make them excellent contenders for next-generation solar cells.
Understanding the fundamental optical properties, such as absorption and emission characteristics, is crucial for optimizing their performance and stability in photovoltaic applications. Furthermore, these properties can be fine-tuned by controlling the material's size, shape, and crystallinity, opening up new avenues for tailoring perovskite materials for specific applications [3]. Elastic properties, as determined by Young's modulus and Poisson's ratio, play a crucial role in the mechanical stability and durability of perovskite materials. Investigating the elastic properties of $CsPbI_3$ is essential to predict their mechanical behaviour under different environmental conditions and can guide the design of robust perovskite-based devices [4]. Population analysis and the identification of defect states are critical for refining the stability and efficiency of perovskite materials. $CsPbI_3$ is known to suffer from defects and trap states, which can adversely affect device performance. Investigating the population of defect states and understanding the factors that influence their formation and dynamics is vital for devising strategies to mitigate these issues [5]. Additionally, the cut-off energy, which represents the energy at which the electronic states of the

[DOI: 10.22068/ijmse.3898]

material are truncated, is an essential parameter for understanding the behaviour of $CsPbI_3$ in different energy regimes. This parameter is critical in the context of electronic band engineering and the utilization of $CsPbI_3$ in various optoelectronic devices [6]. Such types of studies depend on DFT with conventional functionals (e.g. GGA, LDA), there's an upward alarm over the numerical reliability of newer density functional approximations (DFAs). These can suffer from relaxed convergence and require dense quadrature grids for accurate total energies—a factor often overlooked in materials-level computational work. Standardise and authenticate the numerical performance and convergence behaviour of modern DFAs in $CsPbI_3$, to confirm accuracy in predicted optical and electronic properties [7]. In light of the potential of $CsPbI_3$ perovskite materials for an extensive range of applications, a comprehensive investigation into their optical, elastic, density of states, band structure, population analysis, and cut-off energy properties is warranted. For diving deeper into mechanical strain, phase transition and any of the doping/anisotropy impact—perhaps designing a computational study for one of these gaps to grab them [8]. This research aims to address these aspects, providing a deeper understanding of $CsPbI_3$ perovskite materials and contributing to the development of advanced materials for future technology. By exploring these diverse properties, we can pave the way for the design and optimisation of novel perovskite-based devices, providing innovative solutions to the pressing challenges of our time, including energy conversion and storage [9].

2. COMPUTATIONAL PARAMETRIZATION

We must focus on structural optimisation, which is the first critical phase for understanding the $CsPbI_3$ solar perovskite material properties via first principles calculations. The structure of solar perovskite $CsPbI_3$ is shown in Figure 1. The $CsPbI_3$ compounds mature in a cubic perovskite structure, specifically in the $Pm\bar{3}m$ space group with lattice parameters are a= 8.10, a= 8.10 Å, b= 8.45, b= 8.45 Å, and c= 11.88, c=11.88 Å, giving a unit cell volume of 813.53 $Å^3$. The cubic symmetry is confirmed by the 90° angles for α, β, and γ. In this structure, Cs^{1+} ions occupy the 4c Wyckoff positions with coordinates (x= 0.519452, y= 0.439837, z= 1/4) and exhibit an 8-coordinate bicapped square prism geometry with Cs to I bond distances ranging from 3.70 to 4.01 Å. Pb^{2+} ions are located at the 4b Wyckoff positions (x= 0.5, y= 0, z= 0.5), forming corner-sharing PbI_6 octahedra with a consistent Pb-I bond length of 3.01 Å and octahedral tilt angles between 19° and 27°. The I^{1-} ions are in two inequivalent sites: the first I site at 4c positions (x= 0.559665, y= 0.993741, z= 3/4) with a slanted see-saw-similar geometry bonded to two Cs atoms and two Pb atoms, and the following I site at 8d positions (x= 0.802792, y= 0.201022, z= 0.031701) forming distorted corner and edge-sharing ICs_3Pb_2 trigonal bipyramids bonded to three Cs and two Pb atoms. This compound has a density of 4.73 g/cm^3 and exhibits semiconducting behaviour, characterised by a 2.01 eV band gap. $CsPbI_3$ is non-magnetic with a total magnetization of 0.00 μB per formula unit, an energy above hull of 0.005 eV/atom indicating near thermodynamic stability, and a predicted formation energy of -1.682 eV/atom. The Cs^+ ions have a bicapped square prism coordination characterized by a coordination sequence index (CSM) of 10 and a value of 3.105, while the Pb^{2+} ions are in an octahedral coordination with a CSM index of 6 and a value of 0.021. This structural and electronic configuration confirms the material's stability and potential for applications in various fields. The prerequisite properties are calculated by the Cambridge Assembly Serial Total Energy Package (CASTEP) software [10].

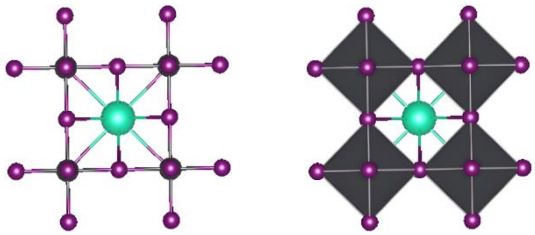

(a) (b)

Fig. 1. Cubic structure of $CsPbI_3$: a) bonded without polyhedral and b) bonded with polyhedral

3. RESULTS AND DISCUSSION

3.1. Structural optimization Using K-Point and Cut-off Energy Variation

To explore the reliance of k-point summation and cut-off energies, we have optimised the structure with several k-point grids and cut-off energies

[DOI: 10.22068/ijmse.3898]

for finding the cell volume with the lowest derivatives. We have changed the cut-off energy from 300 eV to 600 eV here. As a result of this change, we get different values for different cut-off energies. But for convenience, we have worked with a cut-off energy value of 400, where we get the lowest deviation value of 2.95869 highlighted in italic text as shown in Table 1.

K-point sampling involves selecting a fixed number of k-points to approximate the integration of the Brillouin zone. The optimal number of k-points influences the precision and efficiency of DFT calculations. Increasing the number of k-points leads to a more precise representation of the electronic structure, but also increases the computational cost. Fewer k-points can speed up calculations but may sacrifice accuracy. We have selected the K point value of 5 5 5 among the others for the accuracy of our work. Using the mentioned k-point values, we obtained the lowest deviation of 3.01825, highlighted in italic text, as shown in Table 2.

By getting these standard values of k-points summation and cut-off energy, it may confirm a more accurate optimised structure for calculating the required properties of $CsPbI_3$ materials.

3.2. Electronic Properties

The crucial factors of inorganic $CsPbI_3$ materials are their electronic structures, where sunlight absorption serves as a light gatherer in DSCs [11]. To understand the metallic, semiconducting, or insulating conditions of a material, it is essential to know the parameters of the electronic band structure, partial density of states (PDOS), and total density of states (TDOS) [12-13]. The energy band structures were calculated along with special lines of high-symmetry points in the first Brillouin zone to gain a deeper understanding of the physical bonding characteristics of the $CsPbI_3$ compound. The calculated band structures at 0 and 15 GPa are presented. For calculating the band structure, a path of the highest symmetry points, X, R, M, and G, is used. The valence band maximum (VBM) and conduction band minimum (CBM) are positioned at the same high symmetry R point as shown in Figure 2. The internal coordinates points of (0.254, 0), (0.434, -1.98), (0.689, -3.73) in the first Brillouin zone are the respective CBM and VBM. The dashed line indicates the Fermi level. Conduction bands are the bands above the Fermi energy level, whereas the lower ones are valence bands. The cubic phase of $CsPbI_3$ appears to have a direct band gap, with the point R, the highest symmetrical point of the Brillouin zone. The crystal structure influences the dispersion of the electronic bands in $CsPbI_3$, plus the interaction between atoms. DFT calculations can determine the specific shape and characteristics of the bands in the Brillouin zone. The structural properties have a significant impact on bandgap energies, highlighting the importance of using accurate geometry [14].

$CsPbI_3$ exhibits a direct bandgap, with an estimated energy of 1.58 eV, calculated from the total density of states (TDOS) using the PBE/GGA functional (see Fig. 3), which is approximately harmonised with experimental data [15]. The electronic properties of atoms and their orbitals are calculated using total and partial density of states.

Table 1. Cut off energy variation for getting the lowest derivative cell volume

Cut off energy	Initial volume	Final volume	Deviation (%)
300	210.644875	217.306841	3.16265
350	210.644875	217.408088	3.21071
400	210.644875	216.877209	2.95869
450	210.644875	217.192933	3.10857
500	210.644875	217.001447	3.01767
550	210.644875	217.148432	3.08745
600	210.644875	217.319806	3.16880

Table 2. K-point variation for getting the lowest derivative cell volume

K-points	Initial volume	Final volume	Deviation (%)
5 5 5	210.644875	217.002679	3.01825
6 6 6	210.644875	217.178760	3.10184
7 7 7	210.644875	217.402854	3.20823
8 8 8	210.644875	217.421634	3.21714
9 9 9	210.644875	217.354195	3.18513

[DOI: 10.22068/ijmse.3898]

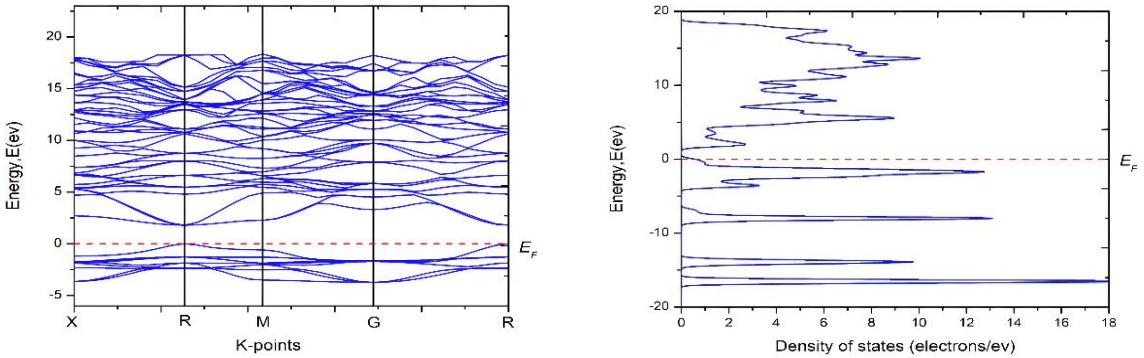

Fig. 2. Band structure (left side) and corresponding band DOS (right side) of $CsPbI_3$ material

To further explain the electronic band structure nature, PDOS of $CsPbI_3$ under 0 and 15 GPa are shown in Fig. 3. The states close to the valence band top are consequent from Cs 4S and Pb 3P orbitals, and the lowest conduction band is composed of I 3d. The electrons in the f state provide very little energy to the $CsPbI_3$ structure, and the maximum energy state density at the Fermi level of $CsPbI_3$ comes from the contribution of the p-orbital electrons, as shown in Figure 3.

3.3. Optical Properties

The dielectric constant-related parameters, including absorption coefficient, reflectivity spectrum, refractive index, and extinction coefficient, can significantly influence the optical properties of materials. Using photon energy ranging from 0 to 40 eV we calculated the absorption coefficient (α (ω)), reflectivity (R (ω)), refractive index (n (ω)) and extinction coefficient (k (ω)) at 0, 10, and 15 GPa.

$CsPbI_3$ is a type of perovskite material that has brought in significant attention due to its remarkable optical and electronic properties. The absorption spectrum has been analysed to determine the optical band gap of $CsPbI_3$.This is a critical parameter for understanding and optimizing its performance in optoelectronic applications. The absorption spectrum can indicate the presence of impurities or deviations in the material's stoichiometry, which could affect its optical properties and overall performance. Absorption graphs aid in optimising layer thickness and composition to maximise light absorption and conversion efficiency. Absorption spectra provide insights into the transition states and electronic structure of $CsPbI_3$. This information is crucial for theoretical modelling and the development of further materials.

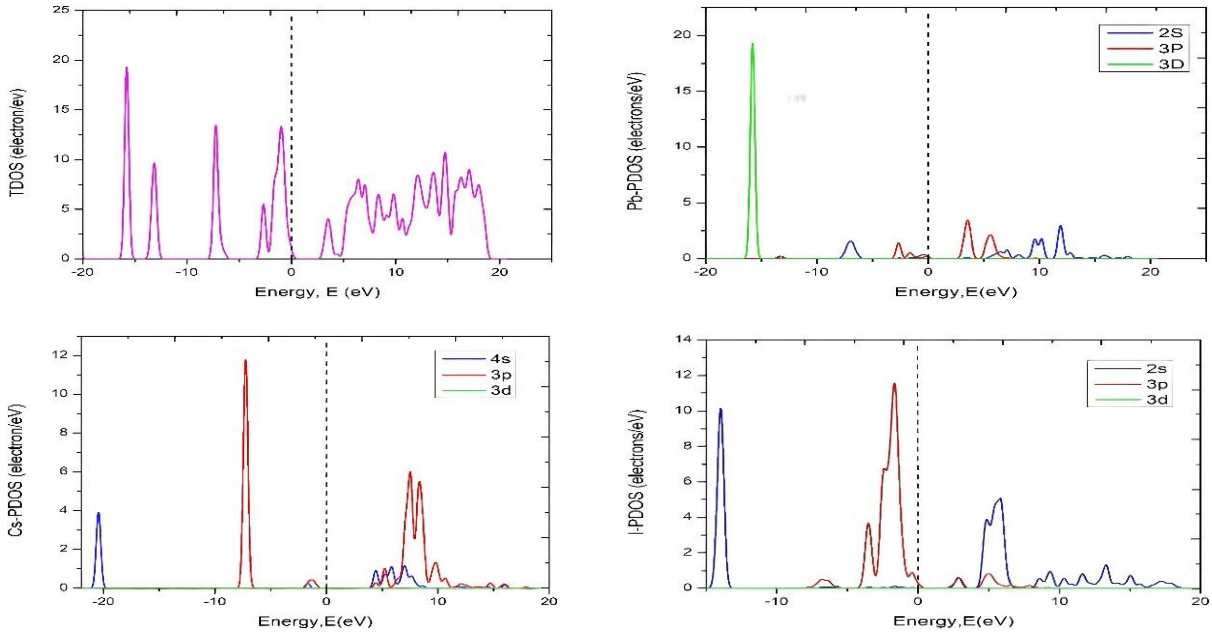

Fig. 3. Total Density of State (TDOS) and Partial Density of States (PDOS) of Cs, Pb and I

[DOI: 10.22068/ijmse.3898]

The overall absorption coefficient decreases with increasing energy. The uppermost absorption peaks for $CsPbI_3$ arose at the energy of 15.1 eV, and the 2nd highest absorption peaks occurred at the energy of 35.1 eV, with the variation of its pressure from zero to 15GPa, as depicted in Figure 4(a). Such a graph of absorption vs. Energy provides a clear and visual representation of how the material interacts with light. Peaks in the absorption spectrum indicate strong light absorption at specific wavelengths, which are related to electronic transitions in the material. In summary, absorption calculations and plotting the optical properties of $CsPbI_3$ are crucial for understanding, optimising, and utilising this material in advanced optoelectronic applications. The complex dielectric function $e(\omega)= e_1(\omega)+ie_2(\omega)$ [ω is the angular frequency] can be used for obtaining the optical properties of the cubic $CsPbI_3$ [16]. The actual alteration between the occupied and unoccupied electric states is typically governed by the imaginary part $e_2(\omega)$. A vital physical parameter is the dielectric function, which labels the optical properties, and reflects the linear response of materials to electromagnetic radiation. [17]. The pressure-varying dielectric function, with its measured real and imaginary parts, is shown in Figure 4(b). The pressure changes from zero to 15 GPa, and the static dielectric constant $e_1(\omega)$ increases from 3.92 to 6.48. The value of $e1(\omega)$ rises from its static value and spreads the main peak, then it starts to decrease significantly. The values of e1 for the main peak are 6.21 at 4.58 eV, 5.21 at 5.87 eV, and 2.58 at 7.65 eV under pressures of 0, 10, and 15 GPa, respectively. The maximum peak value decreases with increasing pressure. The highest peak of $e_2(\omega)$ characterises the strongest absorption of $CsPbI_3$ and drops abruptly with the increasing pressure, as shown in Fig. 4(c). The spectrum shape of e_2 for the cubic $CsPbI_3$ is almost independent on pressure. The two main peaks of e_2 are 5.21 at 5.87 eV, and 2.58 at 7.65 eV under a pressure of 0 GPa. The main peak of the e2 shift moves to lower energy with increased pressure. The higher value of the static dielectric function at low photon energy rapidly decreased with the increase in photon energy. The information on the dielectric function aids in calculating all other optical properties. Optical constants are imperative in designing optical devices.

As pressure increases on cubic $CsPbI_3$, the static refractive index increases, indicating a higher density or a more complex interaction with light. The primary absorption peak shifts to higher energies, suggesting that the bandgap of the material increases under pressure. These changes are consistent with the observed behaviour in other optical properties such as the extinction coefficient and reflectivity [6].

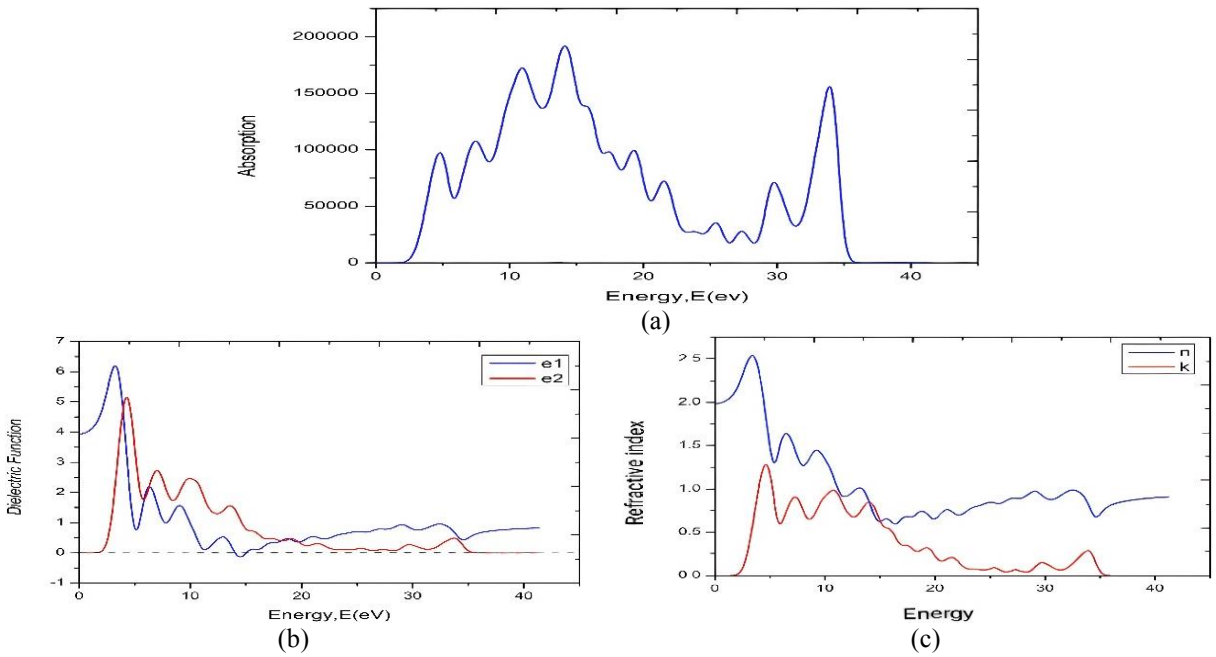

Fig. 4. a) Graph of absorption vs. Energy, b) The measured real and imaginary parts of dielectric function with varying pressure and c) Graph of reflective index vs. Energy

[DOI: 10.22068/ijmse.3898]

The refractive index, often denoted as n, is an optical property of a material that describes how light propagates through it. The refractive index of the CsPbI3 perovskite material plays a crucial role in determining its optical properties and suitability for various applications. The refractive index of $CsPbI_3$ depends on several factors, including the wavelength of light, temperature, and crystal structure. A relatively high refractive index is advantageous for photovoltaic applications because it can help trap and guide light within the material, thereby increasing the chances of photon absorption and conversion into electrical energy. It's essential to note that $CsPbI_3$ can undergo phase transitions under various conditions, including changes in temperature or pressure. These phase transitions can affect its optical properties, including the refractive index. Researchers and engineers working with $CsPbI_3$ perovskite materials must consider these variations in the refractive index when designing and optimizing devices. Understanding how the refractive index changes with different conditions is essential for fitting the material's performance in specific applications. To advance the stability and performance of $CsPbI_3$ perovskite materials, it is necessary to continue research that makes them even more promising for various optoelectronic applications in the future [18].

3.4. Elasticity

The elasticity of $CsPbI_3$ perovskite materials plays a significant role in their characteristics and applications. It affects mechanical, optical, and electronic properties, as well as their suitability for specific uses. Researchers and engineers must consider the elasticity of these materials when designing and using them in various applications, from photovoltaics to optoelectronics. Here, we obtain the values of C11, C44, and C12 as follows. Taylor expansion of the total energy express the elastic constants, the strained system energy is stated as follows:

$U(V,\delta) = U(VV0,0) + VV0[\sum iiii\ \tau\tau ii\delta\delta ii\xi\xi ii + 0.5\ \sum iiii\ CCiiii\delta\delta ii\xi\xi ii\delta\delta jj\xi\xi jj]$,

where $U(VV0, 0)$ is the energy of the opaque system with equilibrium volume $VV0$, $\tau\tau ii$ is an element in the stress tensor, and $\xi\xi ii$ is a factor to take care of Voigt index 22. For the cubic compound $CsPbI_3$, there are nine independent elastic constants (C11, C44, C12). It requires nine strains to find them, which are summarised in Table 3. The elastic properties gained in this work should serve as a good reference for further inquiry, given the absence of any theoretical and experimental data [12].

Table 3. Summary of elastic constants

Cij	Value (GPa)
C11	39.53700
C44	5.27885
C12	6.98020

3.5. Population Analysis

For the population analysis of $CsPbI_3$, we determined the values of Cs, Pb, and I separately. The value of charge spilling was 0.15 for each material. The s-p-d values of Cs, Pb, and I were (2.23, 6.03, 0), (2.05, 1.35, 10.0), and (1.86, 5.53, 0), respectively. Through various mathematical analyses, we obtain effective valences of 0.43, 3.40, and 0.61. The mentioned values are shown in Table 4. The highest occupied orbital is the p orbital, and the highest contribution comes from Cs atoms. However, the d orbitals of Cs and I are empty, whereas Pb shows ten times higher contributions than the others—only I in a condition of negative charge value with positive effectiveness.

4. CONCLUSIONS

First-principles-based DFT calculations were carried out to study the electronic and optical properties of cubic perovskite $CsPbI_3$ materials. The lowest derivative of cell volume is used for further calculation of property analysis by choosing a set of k points with summation, 5 x 5 x 5, and a cut-off energy of 400 eV. The electronic properties analysis concluded that cubic $CsPbI_3$ exhibits a direct band gap, with a minimum band gap of about 1.58 eV, where the p and f orbitals contribute the highest and lowest to the electronic state, respectively.

Table 4. Population analysis

Compound	Charge spilling	species	Muliken atomic population				Muliken charge	Formula ionic charge	Effective valence
			S	P	d	Total			
$CsPbI_3$	0.15	Cs	2.23	6.30	0	8.43	0.57	1	0.43
		Pb	2.05	1.35	10.0	13.40	0.60	4	3.40
		I	1.86	5.53	0	7.39	-0.39	-1	0.61

[DOI: 10.22068/ijmse.3898]

Our results concluded that the highest absorption points for $CsPbI_3$ occurred at an energy of 15.1 eV, and this value decreased with increasing energy as the pressure varied from zero to 15 GPa. The maximum peak value of the dielectric constant increased with growing pressure, and the uppermost peak denotes the strongest absorption of $CsPbI_3$, which drops abruptly with increasing pressure. The extinction coefficient (k(ω)) and refractive index (n(ω)) presented the focal peak at the same energy level in pressure variation, which play a crucial role in determining its optical characteristics and its suitability for various applications.

ACKNOWLEDGEMENTS

I'm grateful to all the co-authors for their cordial and logistical support regarding this research.

REFERENCES

[1] Zhao, F., Guo, Y., Wang, X., Tao, J., Li, Z., Zheng, D., Jiang, J., Hu, Z., and Chu, J., "Efficient carbon-based planar $CsPbBr_3$ perovskite solar cells with Li-doped amorphous Nb_2O_5 layer". J. Alloy. Compd., 2020, 842, 1559840. https://doi.org/10.1016/j.jallcom.2020.155984.

[2] Wang, Y., Hu, Z., Yao, W., Yang, C., Zhang, H., Zhang, J., and Zhu, Y., "Heterogeneous photoresponse of individual grain in all-inorganic perovskite solar cells". Appl. Phys. Lett., 2020, 117, 083902–083906. https://doi.org/10.1063/5.0014187.

[3] Xu, W., Gao, Y., Ming, W., He, F., Li, J., Zhu, X., Kang, F., Li, J., and Wei, G., "Suppressing Defects-Induced Nonradiative Recombination for Efficient Perovskite Solar Cells through Green Antisolvent Engineering". Adv. Mater., 2020, 32, 1–10. https://doi.org/10.1002/adma.202003965.

[4] Miyasaka, T., Kulkarni, A., Kim, G.M., Öz, S., and Jena, A., "Perovskite Solar Cells: Can We Go Organic-Free, Lead-Free, and Dopant-Free"? Adv. Energy Mater., 2019, 10, 1–20. https://doi.org/10.1002/aenm.201902500.

[5] Best Research-Cell Efficiency Chart. NREL. 2022. https://www.nrel.gov/pv/cell-efficiency.html.

[6] Duan, J., Zhao, Y., Yang, X., Wang, Y., He, B., and Tang, Q., "Lanthanide Ions Doped $CsPbBr_3$ Halides for HTM-Free 10.14%-Efficiency Inorganic Perovskite Solar Cell with an Ultrahigh Open-Circuit Voltage of 1.594 V". Adv. Energy Mater., 2018, 8, 1–9. https://doi.org/10.1002/aenm.201802346.

[7] L. Gao, Y. Tang, "Theoretical Study on the Carrier Mobility and Optical Properties of CsPbI3 by DFT", ACS Omega 2021, 6, 17, 11545–11555. https://doi.org/10.1021/acsomega.1c00734.

[8] M. Afsari, A. Boochani, M. Hantezadeh; "Electronic, optical and elastic properties of cubic perovskite CsPbI3: Using first principles study", Elsevier, 2016, 127, 23, 11433-11443. https://doi.org/10.1016/j.ijleo.2016.09.013.

[9] Ren, Y., Zhang, N., Arain, Z., Mateen, M., Chen, J., Sun, Y., and Li, Z., "Polymer-induced lattice expansion leads to all-inorganic $CsPbBr_3$ perovskite solar cells with reduced trap density". J. Power Sources., 2020, 475, 228676. https://doi.org/10.1016/j.jpowsour.2020.228676.

[10] Aktary, M., Kamruzzaman, M., and Afrose, R., "Pressure-dependent comparative study of the mechanical, electronic, and optical properties, of $CsPbX_3$ (X= Cl, Br, I): a DFT study for optoelectronic applications". Adv. Mater., 2023, 4, 4494. https://doi.org/10.1039/D3MA00311F.

[11] Burschka, J., Pellet, N., Moon, SJ., Humphry-Baker, R., Gao, P., Mohammad Nazeeruddin K., and Grätzel M, "Sequential deposition as a route to high-performance perovskite-sensitized solar cells". Nature, 2013, 499, 316-320. https://doi.org/10.1038/nature12340.

[12] M. A. A. Asad, M. A. Alim, M. H. Khatun, A. C. Sarker, M. A. Rahman, "Analysis of the Properties of Vacancy Mediated Methyl Ammonium Lead Iodide Perovskite: A DFT Based Study" East European Journal of Physics, 2025, 1, 327-331. https://doi.org/10.26565/2312-4334-2025-1-39.

[13] Yan, J., Hou, S., Li, X., Dong, J., Zou, L., Yang, M., Xing, J., Liu, H., and Hao, H., "Preparation of highly efficient and stable $CsPbBr_3$ perovskite solar cells based on an anti-solvent rinsing strategy". Sol. Energy

[DOI: 10.22068/ijmse.3898]

Mater. Sol. Cells., 2022, 234, 111420–111428. https://doi.org/10.3390/en16186426.

[14] Borriello, I., Cantele, G., and Ninno, D., "Ab initio investigation of hybrid organic-inorganic perovskites based on tin halides". Phys. Rev. B., 2008, 77, 235214. https://doi.org/10.1103/PhysRevB.77.235214.

[15] Wang, Z., Lin, Q., Chmiel, F.P., Sakai, N., Herz, L., and Snaith, H., "Efficient ambient-air-stable solar cells with 2D–3D heterostructured butylammonium-caesium-formamidinium lead halide perovskites". Nat. Energy., 2017, 2, 17135. https://doi.org/10.1038/nenergy.2017.135.

[16] Fu, W., Liu, H., Shi, X., Zuo, L., Li, X., and Jen, A.K., "Tailoring the Functionality of Organic Spacer Cations for Efficient and Stable Quasi-2D Perovskite Solar Cells". Adv. Funct. Mater., 2019, 29, 1–8. , https://doi.org/10.1002/adfm.201900221.

[17] Lee, K., Kim, J., Yu, H., Lee, J.W., Yoon, C.-M., Kim, S.K., and Jang, J., "A highly stable and efficient carbon electrode-based perovskite solar cell achieved via interfacial growth of 2D PEA2PbI4 perovskite". J. Mater. Chem. A., 2018, 6, 24560–24568. https://doi.org/10.1039/C8TA09433K.

[18] Hashin, Z., and Shtrikman, S., "A variational approach to the theory of the elastic behaviour of polycrystals". J. Mech. Phys. Solids., 1992, 10, 335. https://doi.org/10.1016/0022-5096(63)90060-7.

[DOI: 10.22068/ijmse.3898]